Journal of Modern Physics, **2013, 4, 848-854**
doi:10.4236/jmp.2013.46114 Published Online June 2013 (http://www.scirp.org/journal/jmp)

Refractive Features and Diffraction Scattering Patterns Observed in the Elastic Scattering of ^{12}C from ^{12}C at Various Energies

Sh. Hamada[1], N. Burtebayev[2]
[1]Faculty of Science, Tanta University, Tanta, Egypt
[2]Institute of Nuclear Physics, Almaty, Kazakhstan
Email: sh.m.hamada@gmail.com

Received March 25, 2013; revised April 24, 2013; accepted May 17, 2013

ABSTRACT

We have measured the angular distributions for ^{12}C ion beam elastically scattered from ^{12}C target of thickness 17.4 μg/cm^2 at energies 15, 18 and 21 MeV which is close to the Coulomb barrier energy for ^{12}C + ^{12}C nuclear system. The elastic scattering of ^{12}C beam on ^{12}C was analysed also at different energies (139.5, 158.8, 180, 240, 288.6, 300, 360 and 420 MeV) from literature in order to obtain the global optical potential parameters, which could fairly reproduce the experimental data. The experimental results were analysed within the framework of both the optical model and the double folding potential obtained with different density-dependent NN interactions which give the corresponding values of the nuclear incompressibility *K* in the Hartree-Fock calculation of nuclear matter. The agreement between the experimental results and the theoretical predictions in the whole angular range is fairly good.

Keywords: Scattering Patterns; Refractive Features; Elastic Scattering; Optical Model; Double Folding; Density Distribution

1. Introduction

There have been rather extensive differential cross section studies for ^{12}C + ^{12}C nuclear system at different energies [1-7] which have been attempted to be explained theoretically by using both phenomenological and microscopic potentials [6-12]. It is commonly known that ^{12}C + ^{12}C nuclear system is one of the key reactions for better understanding of the formation of heavier elements in nuclear burning process. In this work, we performed the experimental measurements for ^{12}C ion beam elastically scattered from ^{12}C target at low energies close to the Coulomb barrier energy for this nuclear system, and the theoretical calculations were performed using both optical model (OM) and double folding potential (DF). In comparison with the various studies concerned ^{12}C + ^{12}C elastic scattering at high and intermediate energies, we found that, the experimental data at intermediate and high energies displaying the typical Fraunhofer oscillations at forward angles and the symmetrization interference near 90˚, with gross structures in between which one could surmise are due to Airy maxima and minima. Our experimental data at low energies close to the Coulomb barrier energy are displaying the typical Fresnel scattering pattern and the symmetrization interference near 90˚ is clearly observed as the experimental measurements were extended up to angle ~150˚.

2. Experimental Details

The experiments were performed in the cyclotron DC-60 INP NNC located at Institute of Nuclear Physics, Almaty, Kazakhstan. The ^{12}C ion beam was accelerated up to energies 15, 18 and 21 MeV and then directed to ^{12}C target of thickness 17.4 μg/cm^2. The dead time was monitored and kept as constant as possible by changing the spectrometer entrance slits and/or the beam intensity. The angular distributions for ^{12}C(^{12}C,^{12}C)^{12}C nuclear system were measured in the angular range 20˚ - 155˚ in the centre of mass system with an increment $\Delta\theta$ = 2˚. The registration system of nuclear reaction products included electronic components firms *ORTEC* and *CANBERRA* with MAESTRO software for recording and processing of the spectra of nuclear processes. Energy spectra of scattered particles were measured using a silicon surface barrier detector (ORTEC) with a sensitive layer thickness

of 100 μm. The detector was located at a distance of 24 cm from the scattering region and had the opportunity to move in the angular range from 10˚ to 75˚ in the laboratory system. The maximum voltage which could be applied on the detector was 30 volt but, during the experiment it was raised up to 20 volt. The ^{12}C beam passed through three collimators of 1.5 mm diameter and focused on the target to a spot diameter of ≈3.9 mm. In order to minimize the evaporation of the target, the beam current was 30 nA. Spectrum analysis has been done using the program MAESTRO [13]. **Figure 1** shows the spectrum for ^{12}C(^{12}C,^{12}C)^{12}C elastic scattering at angle 35˚ and at energy 18 MeV. Final normalization of the absolute cross sections was determined by comparing the measurements at the most forward angles, where Mott scattering dominates, with optical model predictions which in this angular region are only weakly dependent on potential parameters.

3. Preparation of ^{12}C Target and Thickness Measurements

The ^{12}C target was prepared using the technique of vacuum evaporation by resistance heating of the specimen with a spot electron gun at the facility UVS-2 (universal vacuum system) see **Figure 2**. The preparation chamber was connected with two pumps rotary pump and turbo molecular pump to achieve the desired vacuum (2×10^{-6} torr) inside the chamber. Firstly, we deposited layers of NaCl crystal salt onto glass plates with the aid of tantalum cradle. Then, electron gun is directed to a sample of graphite with ^{12}C concentration of 98% and placed at 3 cm from the electron gun. The size of the beam spot (2 - 3 mm diameter). Under the influence of electrons, the sample is strongly heated, evaporated, and deposited onto glass plates with previously deposited layers of salt which acts as a release agent and facilitates the removal of carbon film. After annealing for 12 hours at 150˚C, the carbon films were removed from the glass plates and placed to specially prepared frames.

The target thickness was carried out using reactions that have narrow and well isolated resonances. For this purpose, the reaction ^{27}Al(p,γ)^{28}Si at $E_{p,\,lab.}$ = 632, 773, 992, 1089 keV [14] was used. After the measurement of the target yield curves over the ^{27}Al(p,γ)^{28}Si resonance at E_p = 992 keV for (an aluminum foil) and for (the ^{12}C target + the aluminum foil) is made, target thicknesses are taken from the shift of the resonance energy obtained by comparing these yield curves as shown in **Figure 3**, these measurements were performed using the resonance chamber in the accelerator UKP-2-1 INP NNC RK located in Almaty, Kazakhstan.

4. Theoretical Analysis

Our experimental results for ^{12}C + ^{12}C nuclear system at

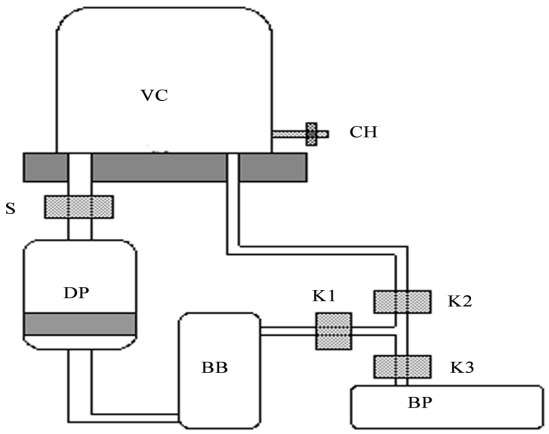

Figure 2. Block diagram of the vacuum system UVS-2; K1, K2, K3: Vacuum Valve; BB: Backing Balloon; S: Manual Vacuum Gate; BP: Backing Pump; VC: vacuum chamber; CH: Vent System; DP: a high-vacuum diffusion pump.

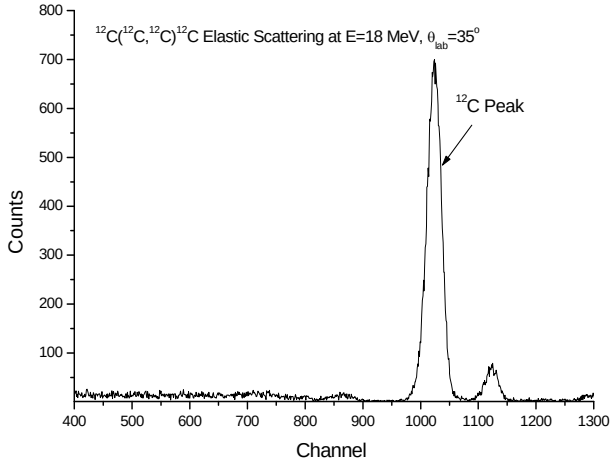

Figure 1. Spectrum for ^{12}C(^{12}C,^{12}C)^{12}C elastic scattering at angle 35˚ and at energy 18 MeV.

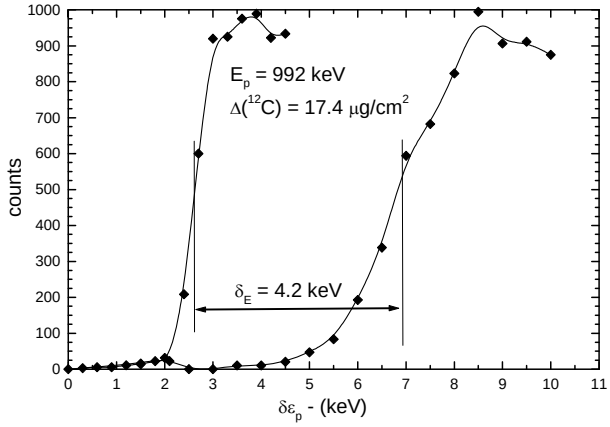

Figure 3. The shift of the 992 keV resonance energy of the ^{27}Al(p,γ)^{28}Si reaction at the expense of the carbon film. The thickness of the ^{12}C target is 17.4 μg/cm^2.

energies 15, 18 and 21 MeV and the experimental data at energies (139.5, 158.8, 180, 240, 288.6, 300, 360 and 420 MeV) from literature [4,15] were analysed (phenomenologically) within the frame work of optical model using Code SPI-GENOA [16] and (semi-microscopically) within the frame work of double folding using code FRESCO [17].

In the phenomenological analyses, Woods-Saxon form factor was taken for both the real and imaginary parts of the potential.

$$\begin{aligned} U &= V_C + V + iW, \\ V &= V_0\left[1+\exp\left(r-R_v\right)/a_v\right]^{-1} \\ W &= W_0\left[1+\exp\left(r-R_w\right)/a_w\right]^{-1} \end{aligned} \quad (1)$$

where, V_0 and W_0, a_v and a_w, R_v and R_w being the depth, diffuseness and radii of the real and imaginary potentials respectively, V_C is the Coulomb potential. The radii are expressed in terms of the target and projectile mass numbers A_t and A_p of the nuclei involved given by

$$R_{v,w} = r_{v,w}\left(A_t^{1/3} + A_p^{1/3}\right) \quad (2)$$

In the double folding calculations, the effective *NN* interaction potential is assumed to have a separable form $v_{\mathrm{D(EX)}}(\rho,s) = F(\rho)v_{\mathrm{D(EX)}}(s)$, where v_{D} and v_{EX} are the direct and exchange terms, respectively, derived from the M3Y interactions [18,19], and s is the inter-nucleon separation; ρ is the density of the surrounding nuclear medium in which the two nucleons are embedded. The radial shape of the M3Y-Paris interaction [18] used in the present folding calculation is given in terms of three Yukawas. The original M3Y interaction is density independent and given in terms of the Yukawa functions as follows:

***M3Y-Reid*:**

$$\begin{aligned} v_{\mathrm{D}}(s) &= 7999.0\frac{\exp(-4s)}{4s} - 2134.25\frac{\exp(-2.5s)}{2.5s}, \\ v_{\mathrm{EX}}(s) &= 4631.38\frac{\exp(-4s)}{4s} - 1787.13\frac{\exp(-2.5s)}{2.5s} \\ &\quad - 7.8474\frac{\exp(-0.7072s)}{0.7072s}, \end{aligned} \quad (3)$$

***M3Y-Paris*:**

$$\begin{aligned} v_{\mathrm{D}}(s) &= 11061.625\frac{\exp(-4s)}{4s} - 2537.5\frac{\exp(-2.5s)}{2.5s}, \\ v_{\mathrm{EX}}(s) &= -1524.25\frac{\exp(-4s)}{4s} - 518.75\frac{\exp(-2.5s)}{2.5s} \\ &\quad - 7.8474\frac{\exp(-0.7072s)}{0.7072s}, \end{aligned} \quad (4)$$

These interactions, especially the M3Y-Reid version, have been used with some success in the double folding model calculation of the HI optical potential at low energies [20], with the elastic data usually limited to the forward scattering angles and, thus, sensitive to the optical potential (OP) only at the surface. However, in cases of refractive (rainbow) nucleus–nucleus scattering where the elastic data are sensitive to the nucleus-nucleus OP over a much wider radial domain, the density-independent M3Y interactions failed to give a good description of the data. The inclusion of explicit density dependence was needed to account for a reduction in the strength of the nucleus-nucleus interaction that occurs at small R where the overlap density of the nuclear collision increases. An early version of the density dependence of the M3Y-Reid interaction was constructed by Kobos *et al.* [21] based upon the *G*-matrix results obtained by Jeukenne *et al.* [22]. It was dubbed as the DDM3Y interaction and has been used to improve the folding model description of the elastic α-nucleus [22,23] and light HI [24] scattering. Hartree-Fock (HF) calculation of the nuclear matter (NM) energy has shown that the original density-independent M3Y interaction Equations (3) and (4) failed to saturate NM, leading to a collapse. The HF method is the first order of nuclear many-body calculation and the introduction of a density dependence into the original M3Y interaction accounts, therefore, for higher order NN correlations which lead to the NM saturation. Several versions of the density dependence of the M3Y-Reid and M3Y-Paris interactions have been introduced by scaling them with an explicit density-dependent function $F(\rho)$. In our present work the density-dependent function $F(\rho)$ was taken in the following form:

$$F(\rho) = C\left[1+\alpha\exp(-\beta\rho) - \gamma\rho^n\right], \quad (5)$$

The parameters C, α, β, γ and n given in **Table 1** were taken from ref. [25].

The nuclear density distribution for ^{12}C was calculated using Three-parameter Fermi model (3PF), where $\rho(r)$ was calculated using the following formula

$$\rho(r) = \rho_0\left(1+\frac{wr^2}{c^2}\right)\Big/\left(1+\exp\left(\left(r-c\right)/z\right)\right)$$

where $w = -0.149$, $Z = 0.5224$ and $c = 2.355$.

5. Theoretical Analysis

The comparison between the experimental data and the theoretical predictions using both optical potential and double folding at energies 15, 18 and 21 MeV is shown in **Figure 4**. In the case of double folding calculations,

Table 1. Parameters of density dependence function $F(\rho)$.

Model	c	α	β(fm^3)	γ(fm^{3n})	n	K(MeV)
CDM3Y6	0.2658	3.8033	1.4099	4.0	1	252

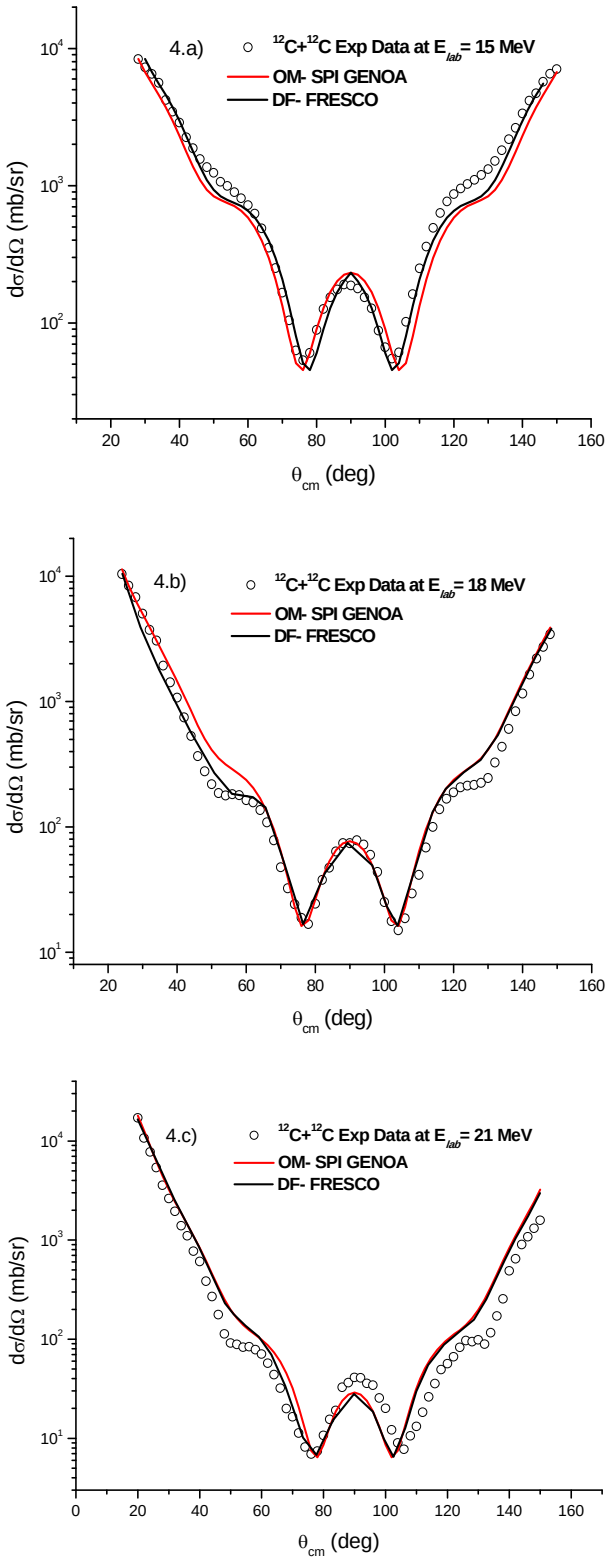

Figure 4. Comparison between experimental and calculated differential cross section within the framework of OM (SPI-GENOA) code and DF (FRESCO) code, for ^{12}C elastically scattered by ^{12}C at energies 15, 18 and 21 MeV respectively.

the normalization factor (*Nr*) equals 1.2. The optical potential parameters for ^{12}C + ^{12}C nuclear system and also those from double folding potential at different energies are listed in **Table 2**. The Coulomb radius parameter rc was fixed at 0.95 fm, the radius parameter for the real part of the potential was fixed at 1.225 fm, the diffuseness parameter for the real part of the potential was fixed at 0.44 fm. While, the radius parameter for the imaginary part of the potential used in the optical model calculations was fixed at 1.294 fm.

In identical particles elastic scattering such as ^{12}C + ^{12}C, due to symmetry under the interchange of spatial coordinates of the two particles, the differential cross section is given by

$$\left(\frac{\mathrm{d}\sigma}{\mathrm{d}\Omega}\right)_{\text{identical}} = \left|f(\theta)+f(\pi-\theta)\right|^2 .$$

where $f(\theta)=f_C(\theta)+f_N(\theta)$, $f(\pi-\theta)=f_C(\pi-\theta)+f_N(\pi-\theta)$, with f_C is the Coulomb scattering amplitude and f_N is the nuclear scattering amplitude. As shown in our experimental results, the total symmetry between cross sections in forward and backward hemispheres tells that the experiments were done correctly.

The comparison between the experimental data and the theoretical predictions using both optical potential and double folding at energies 139.5, 158.8, 180, 240, 288.6, 300, 360 and 420 MeV is shown in **Figures 5** and **6**. The optical potential parameters for ^{12}C + ^{12}C nuclear system and also those from double folding potential at energies (139.5 - 420 MeV) are listed in **Table 3**.

The Coulomb radius parameter r_c was fixed at 0.95 fm, the radius parameter for the real part of the potential was

Table 2. The optimal potential parameters or ^{12}C elastically scattered on ^{12}C at energies 15, 18 and 21 MeV, $R = r_0\left(A_t^{1/3}+A_p^{1/3}\right)$.

E (MeV)	Model	N_r	V_0 (MeV)	W_0 (MeV)	r_W (fm)	a_w (fm)
15.0	OM		99.93	20.54	1.294	0.292
	DF	1.2		40.0	1.0	0.532
18.0	OM		92.98	26.92	1.294	0.3
	DF	1.2		40.0	1.2	0.765
21.0	OM		85.98	29.64	1.294	0.292
	DF	1.2		40.0	1.1	0.4

E (MeV)	Model	J_V (MeV·fm^3)	J_W (MeV·fm^3)
15.0	OM	544.7	127.25
	DF	544.7	126.58
18.0	OM	528.07	198.02
	DF	528.07	182.53
21.0	OM	468.54	183.63
	DF	468.54	157.93

Table 3. The optimal potential parameters for ^{12}C elastically scattered on ^{12}C at different energies, $R = r_0\left(A_t^{1/3} + A_p^{1/3}\right)$.

E (MeV)	Model	N_r	V_0 (MeV)	a_V (fm)	W_0 (MeV)	r_W (fm)	a_W (fm)
139.5	OM		210.0	0.835	20.50	1.21	0.502
	DF	0.68			40.0	0.99	0.589
158.8	OM		195.31	0.836	22.0	1.21	0.503
	DF	0.622			39.9	0.98	0.577
180.0	OM		187.5	0.765	23.80	1.21	0.568
	DF	0.795			22.64	1.13	0.658
240.0	OM		175.0	0.844	27.5	1.21	0.555
	DF	0.907			28.0	1.13	0.680
288.6	OM		158.5	0.878	28.9	1.21	0.785
	DF	0.961			39.99	0.98	0.895
300.0	OM		165.0	0.709	29.0	1.21	0.594
	DF	0.875			25.28	1.1	0.783
360.0	OM		145.0	0.813	29.0	1.21	0.711
	DF	0.708			40.0	0.88	0.961
420.0	OM		125.0	0.668	29.0	1.21	0.872
	DF	0.695			19.43	1.23	0.916

E (MeV)	Model	J_V (MeV·fm^3)	J_W (MeV·fm^3)
139.5	OM	366.34	109.63
	DF	366.34	126.44
158.8	OM	339.29	117.69
	DF	339.29	121.98
180.0	OM	305.21	129.52
	DF	305.21	105.78
240.0	OM	306.38	149.5
	DF	306.38	132.05
288.6	OM	304.54	171.3
	DF	304.54	146.07
300.0	OM	255.56	159.74
	DF	255.56	116.37
360.0	OM	246.68	166.78
	DF	246.68	118.94
420.0	OM	186.93	178.54
	DF	186.93	127.36

fixed at 0.726 fm. At small angles, the cross section is dominated by diffraction and exhibits a typical Fraunhofer diffraction pattern. Beyond this region the cross section exhibits a structureless exponential falloff. Different experiments showed that, there is no evidence of rainbow scattering could be seen in the ^{12}C + ^{12}C system studied at low incident energy [26]. At energies 140 and 159 MeV, the differential cross sections were measured up to 90˚, and it is possible to guess at the presence of broad Airy maxima (centred at ≈50˚ at 159 MeV and at ≈ 62˚ at 140 MeV), in between the Fraunhofer pattern at forward angles and the oscillations near 90˚ due to symmetrization. While the data at 240 and 289 MeV didn't extend far enough to display the full extent of a nuclear rainbow, the measurements at 360 MeV show the beginning of the exponential falloff of the nuclear rainbow, distinctly evident in the angular distribution beyond $\theta_{cm} \approx$ 25˚. As *E/A* approaches 100 MeV and higher, the rainbow moves forward faster than the Fraunhofer oscillations, and the visual identification of its Airy minima in the angular distribution is less clear.

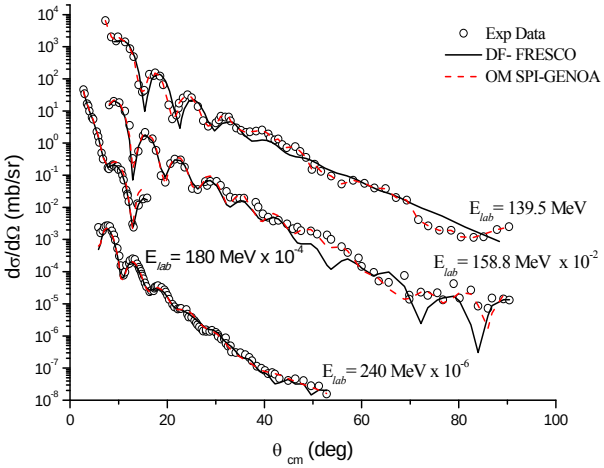

Figure 5. Comparison between experimental and calculated differential cross section for ^{12}C + ^{12}C elastic scattering at energies 139.5, 158.8, 180 and 240 MeV using both OM and DF potentials.

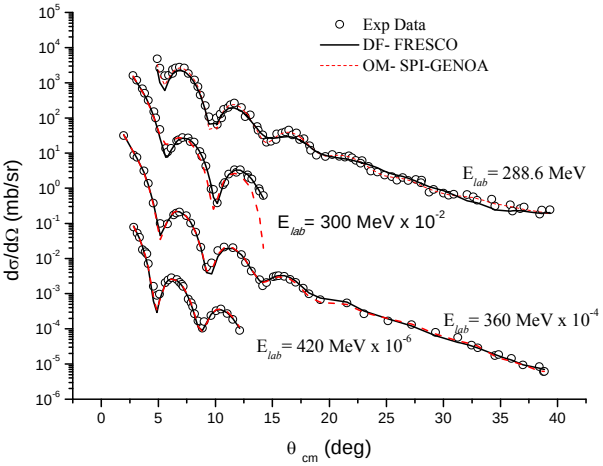

Figure 6. Comparison between experimental and calculated differential cross section for ^{12}C + ^{12}C elastic scattering at energies 288.6, 300, 360 and 420 MeV using both OM and DF potentials.

It has been found that, at incident energies of a few MeV per nucleon, several light heavy-ion systems, among which ^{12}C + ^{12}C display more transparency than most neighboring systems. Indeed, their elastic scattering angular distributions reveal refractive features, such as rainbow scattering patterns and broad interference minima "Airy minima" [27]. These refractive features, can be described consistently only by using the optical potentials with a deep (several hundreds MeV) real part, and the imaginary part of the potential is weak enough to allow some information to transpire from the nuclear interior in the elastic scattering differential cross section: the optical potential displays some *transparency*. The combination of these two features—deep real potential and incomplete absorption—makes possible the observa-

tion in the elastic scattering data of distinctive refractive effects, like strong Airy minima, superimposed on more classic diffractive features. This refractive behavior is clear in the systematic analyses carried out for the ^{16}O + ^{16}O system by Nicoli *et al.* [28] at incident energies between 75 and 124 MeV and by Khoa *et al.* [29] between 124 and 1120 MeV, and for the ^{12}C + ^{16}O system by Nicoli *et al.* [30] between 62 and 124 MeV and by Ogloblin *et al.* [31] at 132 MeV. In particular, we want to clarify the transition between the region of relatively high incident energies where rainbow scattering has set in and lower energies close to Coulomb barrier energy where rainbow scattering is not yet observed. In our present work, it is clearly shown that, refractive features such as; nuclear rainbow phenomenon is not observed in ^{12}C + ^{12}C nuclear system at low energies close to Coulomb barrier energy. The optical model analysis for this nuclear system at low energies near the Coulomb barrier energy doesn't require deep real potential as at high energies.

6. Summary

The angular distributions for ^{12}C ion beam elastically scattered by ^{12}C at energies 15, 18 and 21 MeV have been measured at the cyclotron DC-60. At these energies which are close to the Coulomb barrier energy for ^{12}C + ^{12}C nuclear system (V_{CB} = 17.44 MeV), the ^{12}C + ^{12}C nuclear system doesn't show any refractive features such as rainbow and Airy minimum which is clearly observed for this nuclear system at high energies and the optical model analysis requires deep real potential and shallow imaginary potential. At low energies close to Coulomb barrier energy, rainbow scattering is not observed and the optical model analysis at such low energies doesn't require deep real potential.

The experimental data were analysed within the frame work of both optical model and double folding. The obtained normalization coefficient N_r equals 1.2. The experimental data showed the typical Fresnel scattering pattern and the symmetrization interference near 90˚ is clearly observed, while at high energies, the ^{12}C + ^{12}C nuclear system displaying typical Fraunhofer scattering pattern.

REFERENCES

[1] S. M. Lenzi, A. Vitturi and F. Zardi, *Nuclear Physics A*, Vol. 536, 1992, pp. 168-178. doi:10.1016/0375-9474(92)90252-F

[2] S. M. Lenzi, A. Vitturi and F. Zardi, *Physical Review C*, Vol. 40, 1989, pp. 2114-2123. doi:10.1103/PhysRevC.40.2114

[3] J. Y. Hostachy, *et al*., *Nuclear Physics A*, Vol. 490, 1988, 441-470. doi:10.1016/0375-9474(88)90514-3

[4] C.-C. Sahm, T. Murakami, J. G. Cramer, A. J. Lazzarini, D. D. Leach, D. R. Tieger , R. A. Loveman, W. G. Lynch, M. B. Tsang and J. Van der Plicht, *Physical Review C*, Vol. 34, 1986, pp. 2165-2170. doi:10.1103/PhysRevC.34.2165

[5] M. E. Brandan, *Physical Review Letters*, Vol. 60, 1988, pp. 784-787. doi:10.1103/PhysRevLett.60.784

[6] H. Emling, R. Nowotny, D. Pelte, G. Schrieder and W. Weidenmeier, *Nuclear Physics A*, Vol. 239, 1975, pp. 172-188. doi:10.1016/0375-9474(75)91141-0

[7] W. Treu, H. Fröhlich, W. Galster, P. Dück and H. Voit, *Physical Review C*, Vol. 22, 1980, pp. 2462-2464. doi:10.1103/PhysRevC.22.2462

[8] I. Boztosun and W. D. M. Rae, *Physical Review C*, Vol. 63, 2001, Article ID: 054607. doi:10.1103/PhysRevC.63.054607

[9] F. Michel and S. Ohkubo, *The European Physical Journal A*, Vol. 19, 2004, pp. 333-339. doi:10.1140/epja/i2003-10133-0

[10] M. Freer, M. P. Nicoli, S. M. Singer, C. A. Bremner, S. P. G. Chappell, W. D. M. Rae, I. Boztosun, B. R. Fulton, D. L. Watson, B. J. Greenhalgh, G. K. Dillon, R. L. Cowin and D. C. Weisser, *Physical Review C*, Vol. 70, 2004, Article ID: 064311. doi:10.1103/PhysRevC.70.064311

[11] D. L. Watson, B. J. Greenhalgh, G. K. Dillon, R. L. Cowin and D. C. Weisser, *Physical Review C*, Vol. 70, 2004, Article ID: 064311. doi:10.1103/PhysRevC.70.064311

[12] C. A. Bremner, S. P. G. Chappell, W. D. M. Rae, I. Boztosun, M. Freer, M. P. Nicoli, S. M. Singer, B. Fulton, D. L. Wat-son, B. J. Greenhalgh, G. K. Dillon and R. L. Cowin, *Physical Review C*, Vol. 66, 2002, Article ID: 034 605. doi:10.1103/PhysRevC.66.034605

[13] "MAESTRO®-32 MCA Emulator for Microsoft® Windows® 98, 2000, NT®, and XP® A65-B32 Software User's Manual Software Version 6."

[14] J. W. Bulter, US Naval Research Laboratory, "NRL Report 5282," 1959.

[15] M. E. Brandan, *Physical Review Letters*, Vol. 60, 1988, pp. 784-787. doi:10.1103/PhysRevLett.60.784

[16] F. Perey, "SPI-GENOA: An Optical Model Code," Unpublished, 1975.

[17] I. J. Thompson, *Computer Physics Reports*, Vol. 7, 1988.

[18] G. Bertsch, J. Borysowicz, H. McManus and W. G. Love, *Nuclear Physics A*, Vol. 284, 1977, pp. 399-419. doi:10.1016/0375-9474(77)90392-X

[19] N. Anantaraman, H. Toki, G. F. Bertsch, *Nuclear Physics A*, Vol. 398, 1983, pp. 269-278. doi:10.1016/0375-9474(83)90487-6

[20] G. R. Satchler, W. G. Love, *Physics Reports*, Vol. 55, 1979, pp. 183-254. doi:10.1016/0370-1573(79)90081-4

[21] A. M. Kobos, B. A. Brown, P. E. Hodgson, G. R. Satchler and A. Budzanowski, *Nuclear Physics A*, Vol. 384, 1982, pp. 65-87. doi:10.1016/0375-9474(82)90305-0

[22] J. P. Jeukenne, A. Lejeune and C. Mahaux, *Physical Review C*, Vol. 16, 1977, pp. 80-96. doi:10.1103/PhysRevC.16.80

[23] A. M. Kobos, B. A .Brown, R. Lindsay and G. R. Sat-

chler, *Nuclear Physics A*, Vol. 425, 1984, pp. 205-232. doi:10.1016/0375-9474(84)90073-3

[24] M. E. Brandan and G. R. Satchler, *Nuclear Physics A*, Vol. 487, 1988, pp. 477-492. doi:10.1016/0375-9474(88)90625-2

[25] Dao T. Khoa, W. von Oertzen, H. G. Bohlen and S. Ohkubo, *Journal of Physics G*: *Nuclear and Particle Physics*, Vol. 34, 2007, pp. R111-R116.

[26] R. M. Wieland, R. G. Stokstad, G. R. Satchler and L. D. Rickertsen, *Physical Review Letters*, Vol. 37, 1976, pp. 1458-1461. doi:10.1103/PhysRevLett.37.1458

[27] D. A. Goldberg and S. M. Smith, *Physical Review Letters*, Vol. 33, 1974, pp. 715-718. doi:10.1103/PhysRevLett.33.715

[28] M. P. Nicoli, F. Haas, R. M. Freeman, N. Aissaoui, C. Beck, A. Elanique, R. Nouicer, A. Morsad, S. Szilner, Z. Basrak, M. E. Brandan and G. R. Satchler, *Physical Review C*, Vol. 60, 1999, Article ID: 064608. doi:10.1103/PhysRevC.60.064608

[29] D. T. Khoa, W. von Oertzen, H. G. Bohlen and F. Nuoffer, *Nuclear Physics A*, Vol. 672, 2000, pp. 387-416.

[30] M. P. Nicoli, F. Haas, R. M. Freeman, S. Szilner, Z. Basrak, A. Morsad, G. R. Satchler and M. E. Brandan, *Physical Review C*, Vol. 61, 2000, Article ID: 034609. doi:10.1103/PhysRevC.61.034609

[31] A. A. Ogloblin, D. T. Khoa, Y. Kondo, Yu. A. Glukhov, A. S. Dem'yanova, M. V. Rozhkov, G. R. Satchler and S. A. Goncharov, *Physical Review C*, Vol. 57, 1998, pp. 1797-1802. doi:10.1103/PhysRevC.57.1797

